A Fault Location Algorithm for Transmission Lines with Tapped Leg – PMU Based Approach

Chi-Shan Yu** Chih-Wen Liu* Ying-Hong Lin*

* : Department of Electrical Engineering, National Taiwan University, Taipei, Taiwan
** . Department of Electrical Engineering National Taiwan University, Taipei, Taiwan, and Department of Electrical Engineering, Private Kuan-Wu Institute of Technology and Commerce, Taipei, Taiwan

Abstract--**This work presents a new fault location algorithm for transmission lines with tapped legs. For the transmission lines connected with short interim tapped leg on the midway, the conventional multi-terminals fault location algorithms are inappropriate for these systems. The proposed fault location algorithm only uses the synchronized phasors measured on two-terminals of the original lines to calculate the fault location. Thus, the existing two-terminals fault locator can still be used via adopting the new proposed algorithms. Using the proposed algorithm, the computation of the fault location does not need the model of tapped leg. The proposed algorithm can be easily applied to any type of tapped leg, such as generators, loads or combined systems. EMTP simulation of a 100km, 345 kV transmission line have been used to evaluate the performance of the proposed algorithm. The tested cases include various fault types, fault locations, fault resistances, fault inception angles, etc. The study also considers the effect of various types of tapped leg. Simulation results indicate that the proposed algorithm can achieve up to 99.95% accuracy for most tested cases.**

Index Terms-- **Transmission lines with tapped leg, Fault locator, Synchronized phasor measurement units (PMUs).**

I. INTRODUCTION

The fault location techniques can be mainly classified into one-terminal and multi-terminals based techniques. Generally, the one-terminal based techniques are simple and easy to implement. However, they are always based on certain assumptions, concerning the source impedance (i.e. the exact knowledge of the network topology during fault), fault resistance, loading, and other factors [1]. Furthermore, when multi-terminals network topologies are considered, the one-terminals based techniques are hardly to achieve accurate results. Differently, the multi-terminals based techniques [2-9] use the phasors measured at both terminals of the network to minimize the fault location errors induced from the [1] assumptions in one-terminal based techniques. Thus, more accuracy results can be achieved. Additionally, when multi-terminals network topologies are considered, accuracy fault locations still can be easily calculated via the multi-terminals measurements.

Since the new rights of way for transmission lines are difficult to obtain in Taiwan, transmission lines tapped by a private generating plant or load with relative short transmission lines have existed at Taipower system in recent years. These interim connections will introduce three-terminals transmission lines into the system. Some studies [2-5] have been proposed for fault location calculation of the three-terminals system. However, all of the techniques proposed in those papers need the synchronized phasors measured at all terminals of the system. Thus, when those techniques are used for the tapped lines, new installations are needed to construct those fault locators. However, since the tapped leg is always short and interim, the new installation of fault locators is not necessary and uneconomic. When using the two-terminals based technique [6-9] to calculate the fault location, the model of tapped leg must be constructed to compute the effect of tapped leg. However, sometimes, the model of tapped leg is not easily constructed, such as the nonlinear load model.

To avoid the new installations of fault locators or the model of tapped leg, this work presents a new fault location algorithm installed in existing fault locators. The proposed algorithm only uses the synchronized phasor measured from the synchronized phasor measurement units (PMUs) installed at two terminals of the original transmission lines. Thus, there is no need of new installation in adopting the proposed new algorithm and the proposed algorithm is appropriate to the interim tapped transmission lines. In addition, since the model of tapped leg is not used in the proposed algorithm, the fault location algorithm can be easily extended to any types of tapped leg (such as generator, or load). When two-terminals algorithms are used to calculate the fault location of tapped system, fault locator must decide whether the fault occurs on left side or right side of the tapped leg. In this paper, a selector is presented to choose the correct side of the tapped leg.

The rest of this paper is organized as follows. Section II begins by describing the theory used to determine the fault location of a tapped connected transmission lines. Then, this section proposes a selector for selecting the correct faulted sides with respect to tapped leg and proposes a method of double-checking the input fault types. A 345 kV sample system is used to evaluate the accuracy of the proposed algorithms with respect to different fault types, fault locations, and fault resistance. Next, Section III presents the simulation results of the performance evaluations. These simulation results come from extensive EMTP [12] tested case. Meanwhile, Section IV discusses some special phenomena from the simulation studies in detail. Conclusions are finally made in Section VI.

II. PRINCIPLES

The proposed algorithm is derived using the following assumptions:

1. the fault impedance is pure resistance.

The authors would like to thank the National Science Council of the Republic of China for financially supporting this research under Contract No. NSC 88-2213-E-002-070.

2. the fault type is a prior input.

The assumptions above are common in the literature dealing with the fault location issue.

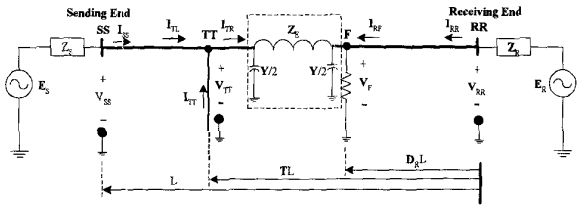

Fig.1 Ground faulted transmission line

A. Fault Location Algorithm

To illustrate the ideas of the proposed algorithms, this work considers the three-phase transposed transmission line with tapped legs shown in Fig.1. The subsystem connected behind the tapped leg can be generators, loads, or combined systems. The tapped leg is connected at a distance of **T** [p.u.] away from the receiving end of the transmission lines and labeled as **TT**. Meanwhile, **SS** and **RR** label the sending and receiving ends of transmission line, respectively. Fig.1 displays that the quantities at each end are all vectors of phase voltages and currents. The long distance distributed transmission line model is used in EMTP simulations and the development of fault location algorithms.

The voltages and currents at a distance x kilometers away from the receiving end are governed by the partial differential equations:

$$\frac{\partial \mathbf{V}}{\partial x} = \mathbf{R}\,\mathbf{I} + \mathbf{L}\frac{\partial \mathbf{I}}{\partial t}$$
$$\frac{\partial \mathbf{I}}{\partial x} = \mathbf{G}\,\mathbf{V} + \mathbf{C}\frac{\partial \mathbf{V}}{\partial t} \qquad (1)$$

where both **V** and **I** are 3 × 1 vectors. **R**, **L**, **G** and **C** are all 3 × 3 transposed line parameters matrices with similar forms such as:

$$\mathbf{L} = \begin{bmatrix} \mathbf{L}_S & \mathbf{L}_M & \mathbf{L}_M \\ \mathbf{L}_M & \mathbf{L}_S & \mathbf{L}_M \\ \mathbf{L}_M & \mathbf{L}_M & \mathbf{L}_S \end{bmatrix} \qquad (2)$$

Under sinusoidal steady-state condition, (1) can be rewritten as

$$\frac{\partial \mathbf{V}}{\partial x} = \mathbf{Z}\mathbf{I}$$
$$\frac{\partial \mathbf{I}}{\partial x} = \mathbf{Y}\mathbf{V} \qquad (3)$$

where $\mathbf{Z} = \mathbf{R} + j\omega\mathbf{L}$ and $\mathbf{Y} = \mathbf{G} + j\omega\mathbf{C}$.

To decouple inter-phase quantities, a suitable transformation, referred to as symmetric component transform [13], is given as follows:

$$\begin{bmatrix} \mathbf{V}_a \\ \mathbf{V}_b \\ \mathbf{V}_c \end{bmatrix} = \mathbf{S}\begin{bmatrix} \mathbf{V}_0 \\ \mathbf{V}_1 \\ \mathbf{V}_2 \end{bmatrix}$$
$$\begin{bmatrix} \mathbf{I}_a \\ \mathbf{I}_b \\ \mathbf{I}_c \end{bmatrix} = \mathbf{S}\begin{bmatrix} \mathbf{I}_0 \\ \mathbf{I}_1 \\ \mathbf{I}_2 \end{bmatrix} \qquad (4)$$

where 0, 1, and 2 respectively represent the zero, positive and negative sequence symmetric components of the voltage and current quantities, and the sequence transformation matrix is as follows:

$$\mathbf{S} = \begin{bmatrix} 1 & 1 & 1 \\ 1 & \alpha^2 & \alpha \\ 1 & \alpha & \alpha^2 \end{bmatrix} \qquad (5)$$

where $\alpha = 1\angle 120°$. Substituting (4) and (5) into (3) gives the following sequence equations:

$$\frac{\partial \mathbf{V}_{012}}{\partial x} = \mathbf{Z}_{012}\mathbf{I}_{012}$$
$$\frac{\partial \mathbf{I}_{012}}{\partial x} = \mathbf{Y}_{012}\mathbf{V}_{012} \qquad (6)$$

where $\mathbf{Z}_{012}$ and $\mathbf{Y}_{012}$ are the sequence impedance and admittance matrices, respectively. Both $\mathbf{Z}_{012}$ and $\mathbf{Y}_{012}$ are diagonal matrices, and the diagonal entries of matrices $\mathbf{Z}_{012}$ and $\mathbf{Y}_{012}$ are ($\mathbf{Z}_0$, $\mathbf{Z}_1$, $\mathbf{Z}_2$) and ($\mathbf{Y}_0$, $\mathbf{Y}_1$, $\mathbf{Y}_2$), respectively. Thus, (6) represents three decoupled sequence systems whose solutions can be obtained as

$$\mathbf{V}_m = \mathbf{A}_m \exp(\gamma_m x) + \mathbf{B}_m \exp(-\gamma_m x)$$
$$\mathbf{I}_m = [\mathbf{A}_m \exp(\gamma_m x) + \mathbf{B}_m \exp(-\gamma_m x)]/\mathbf{Z}_{cm} \qquad (7)$$

where the subscript m denotes 0, 1 and 2 sequence variables, $\mathbf{Z}_{cm} = \sqrt{\mathbf{Z}_m/\mathbf{Y}_m}$ denotes the characteristic impedance, and $\gamma_m = \sqrt{\mathbf{Z}_m\,\mathbf{Y}_m}$ is the propagation constant. Meanwhile, the constants $\mathbf{A}_m$ and $\mathbf{B}_m$ can be determined by the boundary conditions of voltages and currents measured at both ends of the line.

Since the fault location with respect to the tapped leg is unknown prior to fault location calculation, the proposed fault location algorithm will first calculate two locations via subroutines 1 and 2 simultaneously. These two faults are assumed to occur at right and left sides of the tapped leg, respectively. Then, a selector is developed for exactly distinguishing the true fault side.

Subroutine 1 — Fault location for the right side of the tapped leg

In this subroutine, Fig.1 is still used for investigation. Fault location is assumed to be located on right side of tapped leg at a distance of $\mathbf{D}_R$ [p.u.] away from the receiving end of transmission lines and labeled as **F**, where subscript R denotes the variables defined on right side of tapped leg. Meanwhile, the tapped leg is connected at a distance of **T** [p.u.] away from the receiving end of the transmission lines and labeled as **TT**. The transmission lines in Fig.1 are divided into two line sections with respect to the tapped leg. Both of them can be regarded as transmission lines without tapped leg. When the voltages $\mathbf{V}_{TT}$ on tapped leg and currents $\mathbf{I}_{TR}$ on right side of tapped leg are known, fault location $\mathbf{D}_R$ can be calculated using conventional two-terminals techniques [6-9]. The voltages $\mathbf{V}_{TT}$ on tapped leg and transmission line current $\mathbf{I}_{TL}$ on left side of tapped leg can be calculated using the line section between **SS** and **TT** incorporates with the boundary conditions of $\mathbf{V}_{SS}$ and $\mathbf{I}_{SS}$. However, due to the uncertainties of tapped leg, the injection currents $\mathbf{I}_{TT}$ from tapped leg are unknown and the transmission line current $\mathbf{I}_{TR}$ on right side of tapped leg are also unknown. Thus, the conventional two-terminals techniques can't be directly used in this system.

In this work, the Gauss-Seidel numerical method is used to calculate the fault location. In the line section between

tapped leg and receiving end, the unknown variables are currents $\mathbf{I}_{TR}$ and fault location $\mathbf{D}_R$ (or fault resistance $\mathbf{R}_{FR}$, fault voltage $\mathbf{V}_{FR}$). Using a two-ports model to represent the line section between **TT** and **F**, the resulting diagram is illustrated in Fig.2. According the circuit theory and assumption constraint, two groups of equations are obtained as follows:

Group-1: Network equations

$$F_1(\mathbf{I}_{TR}, \mathbf{D}_R, \theta)=0$$

Group-2: Constraint equations

$$F_2(\mathbf{I}_{TR}, \mathbf{D}_R, \theta)=0$$

where θ are the known variables, such as $\mathbf{V}_{SS}$, $\mathbf{V}_{RR}$, $\mathbf{V}_{TT}$, etc., and $\mathbf{I}_{TR}$, $\mathbf{D}_R$ are the unknown variables. Group-1 equations are obtained from the two-ports network enclosed by dashed line in Fig.1. Group-2 equations are obtained from the assumption of pure resistance fault impedance. Since the simultaneous equations of Group-1 and Group-2 are nonlinear, numerical method [14] is needed to find the solutions of $\mathbf{I}_{TR}$ and $\mathbf{D}_R$.

In this work, the Gauss-Seidel numerical method is used. The calculating procedures are arranged as follows:

1. Give an initial value of $\mathbf{D}_R^1$ (superscript 1 denotes the initial value of the first iteration).
2. Substitute $\mathbf{D}_R^1$ into Group-1 equations to calculate $\mathbf{I}_{TR}^1$.
3. Substitute $\mathbf{I}_{TR}^1$ into Group-2 equations to calculate $\mathbf{D}_R^2$.
4. Repeat steps 2 and 3 to calculate the final results of $\mathbf{I}_{TR}$ and $\mathbf{D}_R$.

For saving the space, only the three-phase-shorted fault is adopted as the example to demonstrate the above procedures. Other types of faults can also be easily calculated via the proposed procedures.

Three-Phase-Shorted Fault:

Group-1 equations:

$$\mathbf{V}_{F1}-\frac{\mathbf{V}_{RR1}+\mathbf{I}_{RR1}\mathbf{Z}_{C1}}{2}\exp(\gamma_1 \mathbf{D}_R \mathbf{L}) + \frac{\mathbf{V}_{RR1}-\mathbf{I}_{RR1}\mathbf{Z}_{C1}}{2}\exp(-\gamma_1 \mathbf{D}_R \mathbf{L}) = 0 \quad (8)$$

$$\mathbf{I}_{TR1}-(\mathbf{V}_{TT1}-\mathbf{V}_{F1})/\mathbf{Z}_{E1}+\mathbf{V}_{TT1}\times\mathbf{Y}_1/2 = 0 \quad (9)$$

$$\mathbf{I}_{F1}+[\frac{\mathbf{V}_{RR1}+\mathbf{I}_{RR1}\mathbf{Z}_{C1}}{2}\exp(\gamma_1 \mathbf{D}_R \mathbf{L}) - \frac{\mathbf{V}_{RR1}-\mathbf{I}_{RR1}\mathbf{Z}_{C1}}{2}\exp(-\gamma_1 \mathbf{D}_R \mathbf{L})]\mathbf{Z}_{C1}^{-1} - [\frac{\mathbf{V}_{TT1}+\mathbf{I}_{TR1}\mathbf{Z}_{C1}}{2\exp(\gamma_1 \mathbf{TL})}\exp(\gamma_1 \mathbf{D}_R \mathbf{L}) - \frac{\mathbf{V}_{TT1}-\mathbf{I}_{TR1}\mathbf{Z}_{C1}}{2\exp(\gamma_1 \mathbf{TL})}\exp(-\gamma_1 \mathbf{D}_R \mathbf{L})]\mathbf{Z}_{C1}^{-1} = 0 \quad (10)$$

Group-2 equations:

$$\mathbf{Re}\{\mathbf{I}_{F1}(\mathbf{D}_R)\}\times \mathbf{Im}\{\mathbf{V}_{F1}(\mathbf{D}_R)\} - \mathbf{Re}\{\mathbf{V}_{F1}(\mathbf{D}_R)\}\times \mathbf{Im}\{\mathbf{I}_{F1}(\mathbf{D}_R)\} = 0 \quad (11)$$

where subscript 1 denotes the positive sequence components. $\mathbf{Re}\{\bullet\}$ and $\mathbf{Im}\{\bullet\}$ respectively denote the real part and imaginary part, (8)-(10) are obtained from transmission lines network model, (11) is obtained from the fault impedance assumption, and $\mathbf{V}_{T1}$ is expressed as

$$\mathbf{V}_{TT1}=\frac{\mathbf{V}_{SS1}+\mathbf{I}_{SS1}\mathbf{Z}_{C1}}{2}\exp[\gamma_1(1-\mathbf{T})\mathbf{L}] + \frac{\mathbf{V}_{SS1}-\mathbf{I}_{SS1}\mathbf{Z}_{C1}}{2}\exp[-\gamma_1(1-\mathbf{T})\mathbf{L}] \quad (12)$$

Using the above two groups equations and the procedures mentioned above, fault location of $\mathbf{D}_R$ can iteratively be calculated.

Subroutine 2 — Fault location for the left side of the tapped leg

When the fault occurs on the left side of the tapped leg, substituting the relations $\mathbf{V}_{SS}=\mathbf{V}_{RR}$, $\mathbf{V}_{RR}=\mathbf{V}_{SS}$, $\mathbf{I}_{SS}=-\mathbf{I}_{RR}$ and $\mathbf{I}_{RR}=-\mathbf{I}_{SS}$ into the above equations, and thus obtaining a new per-unit fault location (denoted as $\mathbf{D}'$) in relation to the reference $\mathbf{x} = \mathbf{L}$. When $x = 0$ is taken as the reference point, the final per-unit fault location can be computed from $\mathbf{D}_L = 1 - \mathbf{D}'$, where subscript L denotes the variables defined on left side of tapped leg.

So far the proposed scheme has only generated two solutions of $\mathbf{D}_R$ and $\mathbf{D}_L$, and which one is the exact fault location remains undetermined. A selector that can easily resolve the mentioned problem will be overlooked here and dealt with later.

B. Fault Side Selector

The resulting solutions of $\mathbf{D}_R$ and $\mathbf{D}_L$ can be divided into the following five conditions:

1. Both $\mathbf{D}_R$ and $\mathbf{D}_L$ are fix values $\in$ [**T**, 0].
2. Both $\mathbf{D}_R$ and $\mathbf{D}_L$ are fix values $\in$ [1, **T**].
3. $\mathbf{D}_R$ cannot be found and $\mathbf{D}_L$ is a fix value $\in$ [1, **T**].
4. $\mathbf{D}_L$ cannot be found and $\mathbf{D}_R$ is a fix value $\in$ [**T**, 0].
5. $\mathbf{D}_R \in$ [**T**, 0], and $\mathbf{D}_L \in$ [1, **T**].

Since the computation of fault locations $\mathbf{D}_R$ and $\mathbf{D}_L$ bases on the assumptions: $\mathbf{D}_R \in$ [**T**, 0]and $\mathbf{D}_L \in$ [1, **T**], the solutions of $\mathbf{D}_L$ and $\mathbf{D}_R$ in condition 1 and condition 2, respectively, violates the assumption. Meanwhile, both condition 3 and condition 4 have only one feasible solution, respectively. Thus, the correct solutions of condition 1 to condition 4 can be easily chosen. However, the selecting of condition 5 remains confusedly. The proposed selector is dedicated for this case. In our investigations, in condition 5, the fault resistance $\mathbf{R}_F$ of the correct side is positive, and the fault resistance of the incorrect side is negative. Therefore, the selecting criterion for condition 5 can be obtained as follows:

The fault location of the calculated set [$\mathbf{D}_R$, $\mathbf{D}_L$] that corresponds to positive $\mathbf{R}_F$ is selected as the correct solution.

C. Demonstration of Fault Side Selector

Herein, the proposed selector is proved via the short distance transmission lines model shown in Fig.2. The tapped leg is connected at a distance of **T** [p.u.] away from the receiving end of the transmission lines and labeled as **TT**. The subsystem connected behind the tapped leg can be generator or load. Fault is assumed occurs at the right side of the tapped leg. The per-unit fault location **D** [p.u.] is the correct fault location and the per-unit fault location **D′** [p.u.] is assumed to be the incorrect fault location, where the fault location **D** and **D′** are on the right side and left side of tapped leg, respectively. Using KVL, the relations of $\mathbf{V}_{SS}$ and $\mathbf{V}_{RR}$ are obtained as follows:

$$V_{SS}=(1-T)LZ_L I_{SS}+(T-D)LZ_L(I_{SS}+I_{TT})+V_F$$
$$=(1-T)LZ_L I_{SS}+(T-D)LZ_L(I_{SS}+I_{TT})+(I_{SS}+I_{RR}+I_{TT})R_F$$
$$=(1-D')LZ_L I_{SS}+V'_F$$
$$=(1-D')LZ_L I_{SS}+(I_{SS}+I_{RR}+I'_{TT})R'_F \quad (13)$$

$$V_{RR}=TLZ_L I_{RR}+(D'-T)LZ_L(I_{RR}+I'_{TT})+V'_F$$
$$=TLZ_L I_{RR}+(D'-T)LZ_L(I_{RR}+I'_{TT})+(I_{SS}+I_{RR}+I'_{TT})R'_F$$
$$=DLZ_L I_{RR}+V_F=DLZ_L I_{RR}+(I_{SS}+I_{RR}+I_{TT})R_F$$

$$V_{RR}=TLZ_L I_{RR}+(D'-T)LZ_L(I_{RR}+I'_{TT})+V'_F$$
$$=TLZ_L I_{RR}+(D'-T)LZ_L(I_{RR}+I'_{TT})+(I_{SS}+I_{RR}+I'_{TT})R'_F$$
$$=DLZ_L I_{RR}-V_F=DLZ_L I_{RR}+(I_{SS}+I_{RR}+I_{TT})R_F \quad (14)$$

rewriting (13) as

$$0=(D'-T)LZ_L I_{SS}+(T-D)LZ_L(I_{SS}+I_{TT})$$
$$+(I_{SS}+I_{RR}+I_{TT})R_F-(I_{SS}+I_{RR}+I'_{TT})R'_F \quad (15)$$

Meanwhile, (14) is rewritten as

$$0=(D'-T)LZ_L(I_{RR}+I'_{TT})+(T-D)LZ_L I_{RR}$$
$$-(I_{SS}+I_{RR}+I_{TT})R_F+(I_{SS}+I_{RR}+I'_{TT})R'_F \quad (16)$$

where $(I_{SS}+I_{RR}+I_{TT})=I_F$ is the fault current of the correct side, $(I_{SS}+I_{RR}+I'_{TT})=I'_F$ is the fault current of the incorrect side. From (15) and (16), the following relation is obtained

$$0=(T-D)I_F+(D'-T)I'_F \quad (17)$$

Since $(T-D)$ and $(D'-T)$ are all positive and real constants, the phase difference between I_F and I'_F must be 180 degrees. Meanwhile, due to the pure resistance assumption on fault impedance, the phase difference between V_F and V'_F must be zero or 180 degrees. The zero degree of phase difference indicates $R_F R'_F<0$ or $R'_F<0$, since R_F must be positive. The 180 degrees of phase difference indicates $R_F R'_F>0$ or $R'_F>0$. From conventional circuit theory, the 180 degrees of phase difference between V_F and V'_F is impossible, since the phase difference between sending end and receiving end is much less than 180 degrees. The possible phase difference between V_F and V'_F is zero degree. Thus, when condition five occurs, the fault location with positive fault resistance is selected as the correct solution.

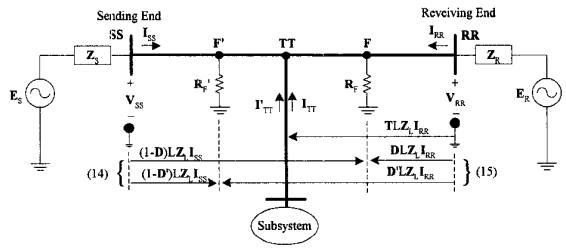

Fig.2 Transmission line for demonstrating selecting algorithm

When the fault occurs at the left side of tapped leg, same results can be obtained by the similar procedures used in above.

D. Fault Location Calculation on Tapped Leg

In this work, the proposed algorithm only concentrates on the fault location calculation of the original transmission lines, and the tapped leg is assumed to be very short or interim. However, when the fault location calculation of the tapped leg is necessary, the fault location still can be calculated via the synchronized measurements from two-terminals of the lines. Before calculation the fault location on tapped leg, the decision of finding whether fault occurs on the tapped leg or the original transmission line. The fault location algorithm proposed in this work incorporate with the two-terminals based fault location algorithm [9] can be used for identifying of this condition. When fault does not occur or fault occurs on the tapped leg, the results calculated from the algorithm proposed in this work cannot be found. In addition, the results calculated from the conventional two-terminals based algorithm [6-9] will equal or near to the tapped leg location. Thus, when both of the above conditions occur, the voltage V_{TT} on tapped leg and the current I_{TT} on tapped leg can be calculated from basic circuit theory and the synchronized boundary conditions of [V_{SS}, I_{SS}, V_{RR}, I_{RR}]. Additionally, the well-known one-terminal based technique [1] can incorporate with the phasors of [V_{TT}, I_{TT}] for fault detection and fault location calculation of the tapped leg

III. PERFORMANCE EVALUATION

A. Algorithm Test

Herein, the proposed fault location algorithm is evaluated via some case studies. The parameters of simulation sample are listed in Table I. Meanwhile, transmission line connects a tapped leg located at 45 km (q = 0.45 p.u.) away from the receiving end of the protected line. All the systems are simulated by EMTP. In order to achieve more accurate results, the phasors are estimated using the SDFT [14-15] filtering algorithm working at 32 samples per cycle. The total simulation time is 200 milliseconds and the error of the fault location is expressed in terms of percentage of total line length. The fault locations, fault resistances and the phase angle of fault currents are computed from subroutine 1 and subroutine 2 simultaneously at 3 cycles after fault inception.

TABLE I. PARAMETERS OF THE SIMULATION SYSTEM

System voltage 345kV	**System frequency** 60Hz
$E_S=1.0\angle 0°$ pu	$E_R=1.0\angle -10°$ pu
$Z_{SA1}=1.31+j15(\Omega)$	$Z_{SB1}=1.31+j15(\Omega)$
$Z_{SA0}=2.33+j26.6(\Omega)$	$Z_{SB0}=2.33+j26.6(\Omega)$
Transmission line parameter : length=100km	
Positive sequence:R=0.0275(Ω/km) L=0.836(mH/km) C=0.021(uF/km)	
Zero sequence : R=0.275(Ω/km) L=2.7233(mH/km) C=0.021(uF/km)	

Generator Type Tapped Leg Tests:

In the following test cases, a generator is connected behind the tapped leg and modeled as a voltage source E_T. The source impedance of E_T is equivalent to that of E_S in Table I. The length of the tapped leg is very short and equal to 5 km.

Case 1:Fault Location Algorithm Test – Small Fault Resistance

A simple case is used to demonstrate the proposed fault location algorithm. Assume that a single-line-to-ground fault occurs at 70 km (D = 0.7 p.u.) away from the receiving end of the line. The fault resistance is assumed to be 1Ω. The phase of E_S leads the phase of E_T by five degrees. The results of subroutine 1 and 2 are written as follows:

Subroutine 1: D_R cannot be found

Subroutine2: $\mathbf{D}_L$=0.7001(p.u.),$\mathbf{R}_F$=1.0274Ω, $\mathbf{Arg}(\mathbf{I}_F)$=1.662(rad)

Since $\mathbf{D}_R$ cannot be found in subroutine 1, the correct fault location is easily chosen as **D**=0.7001 (p.u.) (error=0.01%).

Case 2:Selector Test—Fault occurs at left side of tapped leg

A special case is used to demonstrate the accuracy of proposed selector. Assume that a three-phase-ground fault occurs at 90 km (**D** = 0.9 p.u.) away from the receiving end of the line. The fault resistance is set as 150Ω. The phase of $\mathbf{E}_S$ leads the phase of $\mathbf{E}_T$ by five degrees. The results of subroutine 1 and 2 are written as follows:

Subroutine 1: $\mathbf{D}_R$= 0.1344 (p.u.), $\mathbf{R}_F$=−105.81Ω, $\mathbf{Arg}(\mathbf{I}_F)$=−0.1922(rad)

Subroutine2: $\mathbf{D}_L$=0.8993(p.u.),$\mathbf{R}_F$=150.26Ω, $\mathbf{Arg}(\mathbf{I}_F)$=2.949(rad)

Since the fault resistance is negative in subroutine 1, the correct fault location is chosen as **D**=0.8993 (error=0.07%). Notably, the phase difference of $\mathbf{I}_F$ between subroutine 1 and subroutine 2 is 3.1412(rad), and approximates to 180 degrees. The difference between 3.1412 and 180 degrees (3.1416) is very small and is induced from the short distance transmission lines assumptions in the demonstration of previous section.

Load Type Tapped Leg Tests:

In the following case, a load is connected behind the tapped leg. The length of the tapped leg is also 5 km.

Case 1:Fault Location Algorithm Test − Small Fault Resistance

A simple normal case is used to demonstrate the proposed fault location algorithm. Assume that a line-to-line fault occurs at 30 km (**D** = 0.3 p.u.) away from the receiving end of the line. The fault resistance is set as 1Ω. The load connected behind the tapped leg is modeled as 30MW+21Mvar at nominal voltage. The results of subroutine 1 and 2 are written as follows:

Subroutine1: $\mathbf{D}_R$=0.3001(p.u.),$\mathbf{R}_F$=1.0091Ω, $\mathbf{Arg}(\mathbf{I}_F)$=1.4976(rad)

Subroutine 2:$\mathbf{D}_L$= 0.2936 (p.u.), $\mathbf{R}_F$=−3.73Ω, $\mathbf{Arg}(\mathbf{I}_F)$=−1.6361(rad)

Since $\mathbf{D}_L$ violates the assumption of subroutine 2, the correct fault location is easily chosen as **D**=0.3001 (p.u.) (error=0.01%).

Case 2: Selector Test—Fault occurs at right side of tapped leg

Assume that a three-phase-ground fault occurs at 10km (**D** = 0.1 p.u.) away from the receiving end of the line. The fault resistance is set as 100Ω. To demonstrate the possible of condition 5 in this case, an special but unreasonable load is assumed to be connected behind the tapped leg and modeled as 100MW+70Mvar at nominal voltage. Due to the extremely large power consumption of this load, the tapped leg can still sink current in fault period.

Subroutine1: $\mathbf{D}_R$=0.1001(p.u.),$\mathbf{R}_F$=99.99Ω, $\mathbf{Arg}(\mathbf{I}_F)$=2.6863(rad)

Subroutine 2: $\mathbf{D}_L$= 0.4651 (p.u.), $\mathbf{R}_F$=−4.09Ω, $\mathbf{Arg}(\mathbf{I}_F)$=−0.4549(rad)

Since the fault resistance is negative in subroutine 2, the correct fault location is chosen as **D**=0.1001 (error=0.01%). Notably, the phase difference of $\mathbf{I}_F$ between subroutine 1 and subroutine 2 is 3.1412(rad), and approximates to 180 degrees.

B. Statistical Evaluation

This subsection evaluates the proposed fault location algorithm with over 1000 test cases obtained from the EMTP simulator. It considers different fault types, resistances, locations, and inception angles as statistical tests. Meanwhile, both generator connected tapped leg and load connected tapped leg are considered. The same transmission line model in Table I is still used. The tapped leg connects at 45 km away from the receiving end of the line. For the generator connected tapped leg, the phase of ES leads the phase of ET five degrees. For the load connected tapped leg, the load is modeled as 30MW+21Mvar at nominal voltage. Table II summarizes all of these results. The fault inception angles are 0, 45, 90, 135, and 180 degrees in relation to the zero cross of a-phase voltage. For saving space, all of the fault location errors are calculated as the average errors for different inception angles and different kind of tapped legs. In Table II, variable Ave is the average fault location. For comparison, variable max is the maximum fault location error in ten fault locations. In all cases, the maximum error is 0.6% and the average error is about 0.039%. Additionally, if only considering the fault resistance less and equal 10W, the maximum error reduces to 0.17% and the average error is only 0.014%.

TABLE II. STATISTICAL TESTING OF THE ALGORITHM

Fault Type	R_F	Fault location error (%) 10km	25km	55km	75km	90km
Three Phases To Ground	0.1Ω	ave=0.001 max=0.001	ave=0.007 max=0.012	ave=0.017 max=0.026	ave=0.007 max=0.011	ave=0.001 max=0.001
	1Ω	ave=0.003 max=0.004	ave=0.007 max=0 011	ave=0.010 max=0.015	ave=0.004 max=0.006	ave=0 002 max=0.003
	10Ω	ave=0.009 max=0.01	ave=0.035 max=0.038	ave=0.006 max=0.008	ave=0.014 max=0.015	ave=0.019 max=0.022
	50Ω	ave=0.014 max=0.026	ave=0.16 max=0.25	ave=0.055 max=0.10	ave=0.01 max=0.019	ave=0.009 max=0.016
	100Ω	ave=0.008 max=0.015	ave=0.22 max=0.47	ave=0.083 max=0.16	ave=0.08 max=0.12	ave=0.009 max=0.017
Two Phases To Ground	0.1Ω	ave=0.003 max=0.007	ave=0.009 max=0.021	ave=0.049 max=0.1	ave=0 012 max=0.021	ave=0.003 max=0.005
	1Ω	ave=0.002 max=0.005	ave=0.014 max=0.032	ave=0.037 max=0.063	ave=0.006 max=0.013	ave=0.002 max=0.004
	10Ω	ave=0 001 max=0.002	ave=0.014 max=0.023	ave=0.049 max=0.083	ave=0.008 max=0.022	ave=0.002 max=0.004
	50Ω	ave=0.001 max=0.002	ave=0.011 max=0.027	ave=0 045 max=0.068	ave=0.005 max=0.01	ave=0 001 max=0.002
	100Ω	ave=0.002 max=0.002	ave=0.014 max=0.032	ave=0.047 max=0.080	ave=0.008 max=0.021	ave=0.001 max=0.002
Line To Line	0.1Ω	ave=0.001 max=0.001	ave=0.013 max=0.035	ave=0.038 max=0.057	ave=0.008 max=0.019	ave=0.001 max=0.002
	1Ω	ave=0.002 max=0.003	ave=0.008 max=0.015	ave=0.013 max=0.025	ave=0.041 max=0.056	ave=0.001 max=0.002
	10Ω	ave=0 016 max=0.027	ave=0.021 max=0.034	ave=0.032 max=0.055	ave=0 007 max=0.014	ave=0.011 max=0.015
	50Ω	ave=0.021 max=0.046	ave=0.098 max=0.11	ave=0 19 max=0.28	ave=0.14 max=0.18	ave=0.067 max=0.092
	100Ω	ave=0.05 max=0.12	ave=0.54 max=0.6	ave=0.3 max=0.6	ave=0.09 max=0.16	ave=0.04 max=0.053
Single Line To Ground	0.1Ω	ave=0.020 max=0.040	ave=0.003 max=0.006	ave=0.039 max=0.069	ave=0 014 max=0.019	ave=0.011 max=0.029
	1Ω	ave=0.008 max=0.009	ave=0.008 max=0.012	ave=0.036 max=0.069	ave=0.012 max=0.018	ave=0.009 max=0.021
	10Ω	ave=0.011 max=0.026	ave=0.013 max=0.024	ave=0.065 max=0.17	ave=0.013 max=0.022	ave=0.006 max=0.013
	50Ω	ave=0.001 max=0.018	ave=0.12 max=0.28	ave=0.11 max=0.20	ave=0.055 max=0.090	ave=0.004 max=0.006
	100Ω	ave=0.013 max=0.022	ave=0 15 max=0.25	ave=0.16 max=0 27	ave=0.12 max=0.16	ave=0.007 max=0.011

IV. CONCLUSIONS

This work has successfully proposed a new fault location algorithm for transmission lines with tapped legs. For the transmission lines tapped with a short or interim transmission line, three-terminals fault location algorithms are inappropriate and uneconomic for these systems. The proposed algorithm does not use the real-time measurements of the tapped legs. Thus, the proposed fault location algorithm is appropriate for these systems. Meanwhile, the proposed fault location algorithm does not use the model of the tapped leg in fault period. Thus, the proposed fault locator can be easily applied to transmission lines with any type of tapped leg, such as generator, load or combined systems. To select the correct fault location with respect to the tapped leg, the fault side selector also has been presented in the work. The simulation results show the proposed fault location algorithm and the selector can easily produce and choose accurate fault location result.

V. REFERENCE

[1] L. Eriksson, et al, "An Accurate Fault Locator with Compensation for Apparent Reactance in the Fault Resistance Resulting from Remote-End Infeed," IEEE Trans. on PAS, Vol. PAS-104, No.2, Feb. pp.424-436, 1985.

[2] A. A. Girgis, D. G. Hart. and W. L. Peterson, "A New Fault Location Technique for Two- and Three- Terminal Lines", IEEE Trans on Power Delivery, Vol.7, No.1, January, pp. 98-107, 1992.

[3] R. K. Aggarwal, et. al., "A Practical Approach to Accurate Fault Location on Extra High Voltage Teed Feeders", IEEE Trans., PWRD-8 (3):pp.874-883, 1993.

[4] Abe Masayuki, "Development of a new Fault Location System for Multi-terminals Single Transmission Lines," IEEE Trans., PWRD-10 (1) pp.159-168, 1995.

[5] Qingwu Gong, et al, "A Study of the Accurate Fault Location System for Transmission Line Using Multi-Terminal Signals", IEEE Winter Meeting, 2000.

[6] A. T. Johns, et al, "Accurate Fault Location Technique for Power System Lines", IEE. Proc. Pt.C, Vol.137, pp.395-402, Nov. 1990.

[7] M. Kezunovic, "An Accurate Fault Location Using Synchronized Sampling at Two Ends of a Transmission Line, " Applications of Synchronized Phasors Conference, Washington, DC, 1993.

[8] D. Novosel et al, "Unsynchronized Two-Terminal Fault Location Estimation," IEEE PES Winter Meeting, New York, Jan. 95WM025-7 PWRD, 1995.

[9] J. –A. Jiang et al, "An Adaptive PMU Based Fault Detection/Location Technique for Transmission Lines Part I", IEEE Trans. on PWRD, Vol.15, No.2, pp.486-493, 2000.

[10] J. –Z. Yang and C. –W. Liu, "A precise calculation of power system frequency and phasor", IEEE Transactions on Power Delivery, Vol.15, No.2, pp.494-499, 2000.

[11] J. –Z. Yang and C. –W. Liu, "Complete Elimination of DC offset in current signals for relaying applications", IEEE Winter Meeting, 2000.

[12] Dommel H., Electromagnetic Transient Program, BPA, Portland, Oregon, 1986.

[13] C. A. Gross, Power System Analysis, John Willey, 1986.

[14] John R. Rice, Numerical Methods, Software, and Analysis, Academic Press Inc., San Diego, 1993.

VI. BIOGRAPHIES

Chi-Shan Yu was born in Taipei, Taiwan in 1966. He received his B.S. and M.S. degree in electrical engineering from National Tsing Hua University in 1988 and 1990, respectively. He is a candidate for the Ph.D. degree in the electrical engineer department at National Taiwan University, Taipei, Taiwan. His current research interests are computer relaying and transient stability controller.

Chih-Wen Liu was born in Taiwan in 1964. He received the B.S. degree in Electrical Engineering from National Taiwan University in 1987, and M.S. and Ph.D. degrees in electrical engineering from Cornell University in 1992 and 1994. Since 1994, he has been with National Taiwan University, where he is associate professor of electrical engineering. He is a member of the IEEE and serves as a reviewer for IEEE Transactions on Circuits and Systems, Part I. His main research area is in application of computer technology to power system monitoring, operation, protection and control. His other research interests include GPS time transfer and chaotic dynamics and their application to system problems.

Ying-Hong Lin was born at Taipei, Taiwan, in 1970. He received his B.S. degree in electrical engineering from Taiwan University of Technology in 1995 and M.S. degree from National Taiwan University in 1999. He is a candidate for the Ph.D. degree in the electrical engineer department at National Taiwan University, Taipei, Taiwan. His interested researches are the application of GPS and PMU in power system.